International Journal of Control and Automation
Vol. 9, No. 10 (2016), pp.257-274
http//dx.doi.org/10.14257/ijca.2016.9.10.25

Multi Induction Motor Synchronous Drive System Based on Diagonal Recurrent Neural Network Control

Chong Chen*, Simin Peng, Zhilei Yao and Quanyu Wang

School of Electrical Engineering, Yancheng Institute of Technology
Yancheng 224051 PR China
cc082120@126.com

Abstract

Through the analysis of the mathematical model of multi induction motor synchronous drive system, a new control method based on neural network is proposed and applied into the system.The neural network controller is composed of self-tuning PID controller based on diagonal recurrent neural network (DRNN) and neuron decoupling compensator. The three self-tuning PID controllers are used in the speed and tension control loops respectively, making the system possess stronger adaptive capability and robustness. The neuron decoupling compensator integrates the effect of the three loops and realizes the adaptive decoupling control between speed and tension by training the weights of network to compensate the coupling relation. The experiment results show that, compared with traditional PID control, the control system can obtain optimal parameters according to online identification of the DRNN network, realizing the better decoupling control of speed and tension, and the system has better dynamic, static characteristics and robustness.

Keywords: *neural network; DRNN; decoupling control; synchronous control; multi induction motor system*

1. Introduction

Since controlled objects are more and more complex, the design theory for traditional control system is facing with severe challenges. Especially, as a complex industrial controlled object, there is coupling effect between each variable [1]. If the multi variable controller is designed with common method, as for industrial process, the linear constant and high precision mathematical model is difficult to achieve. Even if achieved, it is also difficult to meet the real industrial control requirements because of its complexity.

Artificial neural network has strong self-learning, adaptive and nonlinear mapping capability. When it is used to design control system, we only need to train the neural network online or offline, and then use the training results without the mathematical model of controlled object. If neural network control method is adopted to control the nonlinear and uncertain system, it will has strong adaptability and robustness. Therefore, artificial neural network can make up for the deficiency of common methods, making the decoupling control of multi variable system possible [2]-[3].

Aiming at the multi induction motor synchronous drive system working under constant V to F, a new neural network compound controller composed of neuron decoupling compensator and self-tuning PID controller is presented in this paper [4]. Based on S7-300 experimental platform, many experiments are carried out and results show that the control system can get optimal parameters according to online identification of the DRNN network, and it realizes the better decoupling control of

ISSN: 2005-4297 IJCA

speed and tension with better performances of dynamic and static status. Thus, the method presented in this paper meets the requirements of many industrial control environments, with good application prospects.

2. Mathematical Model of Multi Induction Motor Synchronous Drive System

The physical model of multi induction motor synchronous drive system is shown in Figure 1. The 1#motor controls line speed, while 2#motor and 3#motor perform the tension control F*. According to the huke laws, the basic dynamic equations can be derived by Eq. (1).In this paper, the tension is proportional to the speed difference between the adjacent two motors in the system [5]-[6].

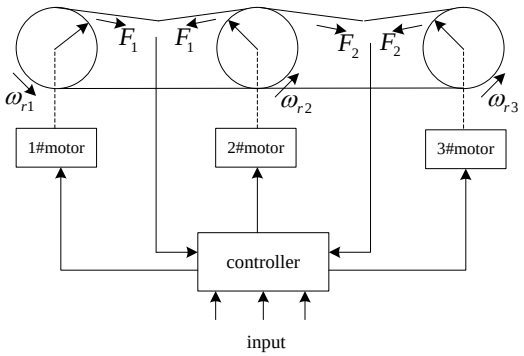

Figure 1. Three Motor Synchronous Drive System

$$\begin{cases} \dot{F_1} = \dfrac{K_1}{T_1}(\dfrac{1}{n_{p1}} r_1 k_1 w_{r1} - \dfrac{1}{n_{p2}} r_2 k_2 w_{r2}) - \dfrac{F_1}{T_1} \\ \dot{F_2} = \dfrac{K_2}{T_2}(\dfrac{1}{n_{p2}} r_2 k_2 w_{r2} - \dfrac{1}{n_{p3}} r_3 k_3 w_{r3}) - \dfrac{F_2}{T_2} \end{cases} \tag{1}$$

Where,

$\omega_{r1}, \omega_{r2}, \omega_{r3}$: 1#motor speed(r/min), 2#motor speed(r/min), 3#motor speed(r/min)

r_1, r_2, r_3: 1#roll radius(m) , 2#roll radius(m), 3#roll radius(m)

k_1, k_2, k_3: speed ratio of 1#roll, speed ratio of 2#roll, speed ratio of 3#roll

n_{P1}, n_{P2}, n_{P3}: 1#motor rotor poles, 2#motor rotor poles, 3#motor rotor poles

T1, T2: time constant of tension variation

K_1, K_2 : transfer coefficient

Laplace transform to Eq. (1) and simplify them as follows：

$$\begin{cases} F_1(s) = (\dfrac{1}{n_{p1}} r_1 k_1 \omega_{r1} - \dfrac{1}{n_{p2}} r_2 k_2 \omega_{r2}) \dfrac{K_1}{T_1 s + 1} \\ F_2(s) = (\dfrac{1}{n_{p2}} r_2 k_2 \omega_{r2} - \dfrac{1}{n_{p3}} r_3 k_3 \omega_{r3}) \dfrac{K_2}{T_2 s + 1} \end{cases} \tag{2}$$

If the motor speed and belt tension are regarded as controlled variables and the given of three inverters as input variables, then open loop control diagram of multi induction motor synchronous drive system can be obtained in Figure 2.

From the above analysis, there is coupling effect among 1#motor speed ω_{r1}, the tension F_1 and F_2, and the affect mutually. Whenever the motor speed or belt tension changes, it will affect the other. Therefore, if we want to realize the synchronous control of the three motors, the decoupling of motor speed and belt tension is needed.

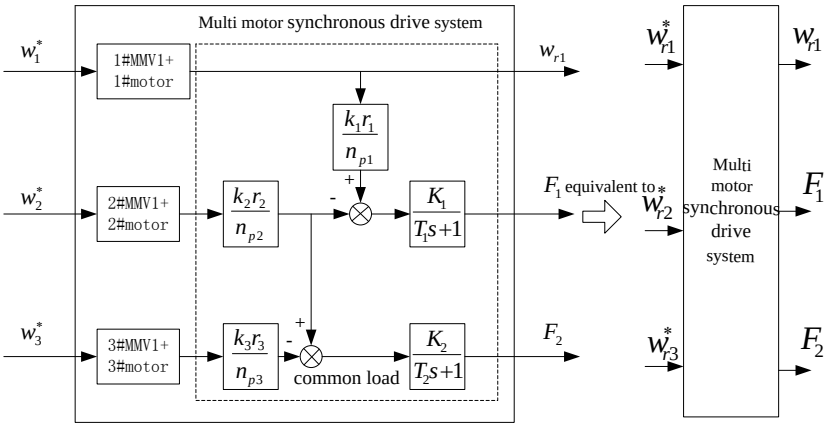

Figure 2. Open Loop Control Diagram of Multi Motor Synchronous Drive System

3. Closed Loop Control of Multi Induction Motor Synchronous Drive System

In order to further improve control performances of multi motor synchronous drive system, neural network control technology is used to design the control system. In order to eliminate the coupling effect between speed and tension loop, neuron decoupling and self-tuning PID control method is adopted to design a new control system. The schematic diagram of control system is shown in Figure.3. The structure is used the series open loop decoupling strategy that the neuron decoupling compensator set behind the self-tuning PID controller [7].

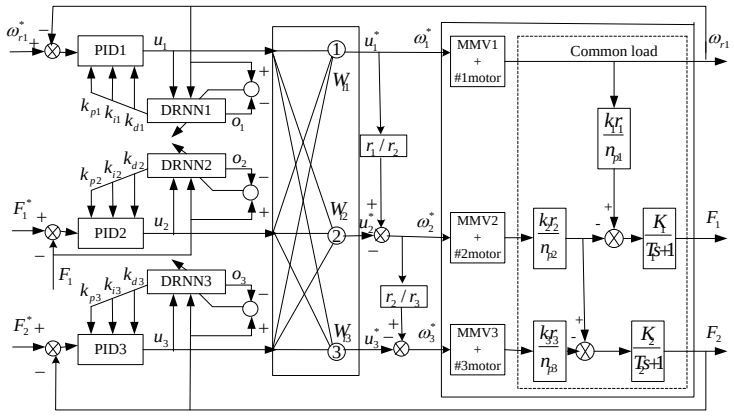

Figure 3. Control Diagram of Multi Motor Synchronous System

3.1. Self-Tuning PID Controller of Speed and Tension Loop

Self-tuning PID controllers based on DRNN are adopted in both speed and tension loops. DRNN is used as on-line identifier. According to the varying environment, It adjusts network weights automatically, and traces the output of controlled object. Jacobian information obtained by DRNN can be used to adjust the parameters of PID controller on-line. This controller has the advantages of fast response, strong adaptability and anti-interference. The principle of self-learning PID controller based on DRNN network is as follows:

Position type PID controller is adopted in this paper. The object is controlled directly in closed loop, and k_P, k_i and k_d are online adjusted [8].

Control algorithm is as follows

$$error(k) = r(k) - y(k) \tag{3}$$

$$\begin{cases} x_1(k) = error(k) \\ x_2(k) = \sum_{i=1}^{k} (error(k) \times T) \\ x_3(k) = \dfrac{error(k) - error(k-1)}{T} \end{cases} \tag{4}$$

$$u(k) = k_p(k)x_1(k) + k_i(k)x_2(k) + k_d(k)x_3(k) \tag{5}$$

Where,

$r(k)$: given speed $\omega_{r1}{}^*$ or input tension F^*

$y(k)$: actual output speed ω_{r1} or output tension f

T: sampling time

Index function can be defined as follows:

$$E(k) = \frac{1}{2}(r(k) - y(k))^2 = \frac{1}{2}e(k)^2 \tag{6}$$

Gradient descent method is adopted to adjust the parameters of k_p, k_i and k_d

$$\begin{cases} E(k) = \dfrac{1}{2}(r(k) - y(k))^2 \\ \Delta k_p = -\eta_p \dfrac{\partial E}{\partial k_p} = -\eta_p \dfrac{\partial E}{\partial y}\dfrac{\partial y}{\partial u}\dfrac{\partial u}{\partial k_p} = \eta_p e(k)\dfrac{\partial y}{\partial u}x_1(k) \\ \Delta k_i = -\eta_i \dfrac{\partial E}{\partial k_i} = -\eta_i \dfrac{\partial E}{\partial y}\dfrac{\partial y}{\partial u}\dfrac{\partial u}{\partial k_i} = \eta_i e(k)\dfrac{\partial y}{\partial u}x_2(k) \\ \Delta k_d = -\eta_d \dfrac{\partial E}{\partial k_d} = -\eta_d \dfrac{\partial E}{\partial y}\dfrac{\partial y}{\partial u}\dfrac{\partial u}{\partial k_d} = \eta_d e(k)\dfrac{\partial y}{\partial u}x_3(k) \end{cases} \tag{7}$$

$\dfrac{\partial y}{\partial u}$ is the Jacobian information of controlled object, which can be obtained by identification of DRNN.

DRNN is a recurrent neural network. It is made of three layers network structure, whose hidden layer is recurrent layer. The 3-7-1 network structure is shown in Figure 4.

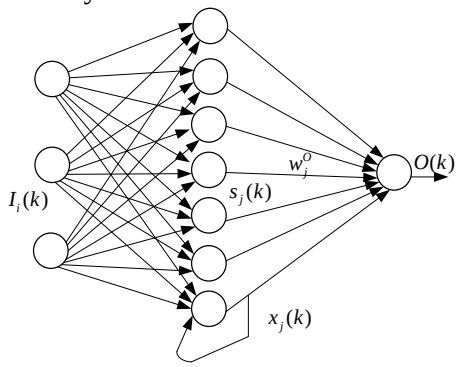

Figure 4. The Structure of DRNN

In DRNN network, $I=[I_1,I_2,...,I_n]$ is set as input vector, and $I_i(k)$ is set as the ith neuron input. In this paper, the input vector of the network is $I=\{u(k-1),y(k),1.0\}$.The algorithm of DRNN is

$$\begin{cases} y_m(k)=O(k)=\sum_j W_j^O X_j(k) \\ X_j(k)=f(S_j(k)) \\ S_j(k)=W_j^D X_j(k-1)+\sum_i W_{ij}^I I_i(k) \end{cases} \tag{8}$$

Where

$X_j(k)$: the jth neuron output of recurrent layer

$S_j(k)$: the jth recurrent neuron input sum

$f(\cdot)$: double S function

$O(k)$, $y_m(k)$: output of DRNN

W^D: weight vector of recurrent layer

W^O: weight vector of output layer

W^I: weight vector of input layer

The identification error is

$$em(k)=y(k)-ym(k) \tag{9}$$

The identification index is

$$Em(k)=\frac{1}{2}em(k)^2 \tag{10}$$

Learning algorithm adopts gradient descent method

$$\begin{cases} \Delta w_j^O(k)=-\dfrac{\partial Em(k)}{\partial w_j^O}=em(k)\dfrac{\partial ym}{\partial w_j^O}=em(k)X_j(k) \\ w_j^O(k)=w_j^O(k-1)+\eta_O\Delta w_j^O(k)+\alpha(w_j^O(k-1)-w_j^O(k-2)) \\ \Delta w_{ij}^I(k)=-\dfrac{\partial Em(k)}{\partial w_{ij}^I}=em(k)\dfrac{\partial ym}{\partial X_j}\dfrac{\partial X_j}{\partial w_{ij}^I}=em(k)w_j^O Q_{ij}(k) \\ w_{ij}^I(k)=w_{ij}^I(k-1)+\eta_I\Delta w_{ij}^I(k)+\alpha(w_{ij}^I(k-1)-w_{ij}^I(k-2)) \\ \Delta w_j^D(k)=-\dfrac{\partial Em(k)}{\partial w_j^D}=em(k)\dfrac{\partial ym}{\partial X_j}\dfrac{\partial X_j}{\partial w_j^D}=em(k)w_j^O P_j(k) \\ w_j^D(k)=w_j^D(k-1)+\eta_D\Delta w_j^D(k)+\alpha(w_j^D(k-1)-w_j^D(k-2)) \end{cases} \tag{11}$$

Double S function of recurrent layer neuron is

$$f(x)=\frac{1-e^{-x}}{1+e^{-x}} \tag{12}$$

$$P_j(k)=\frac{\partial X_j}{\partial w_j^D}=f'(S_j)X_j(k-1) \tag{13}$$

$$Q_{ij}(k)=\frac{\partial X_j}{\partial w_{ij}^I}=f'(S_j)I_i(k) \tag{14}$$

Where

η_I: learning rate of input layer

η_D: learning rate of recurrent layer

η_O: learning rate of output layer

α : inertial coefficient

Jacobian information of the controlled object $\frac{\partial y}{\partial u}$ is

$$\frac{\partial y}{\partial u} \approx \frac{\partial ym}{\partial u} = \sum_j w_j^O f'(S_j) w_{ij}^I \tag{15}$$

3.2. Adaptive Neuron Decoupling Compensator of Multi Variable System

Neuron decoupling compensator views the coupling effect from other channels as measurable disturbances to compensate. It makes the generalized system composed of neuron decoupling compensator and multi motor synchronous drive system into the system without or with a little coupling, by adjusting weights of neuron compensation network. The serial open loop decoupling strategy is adopted in this paper, that is, decoupling compensator is set behind controller. A single neuron is set in every pair input and output channel. Each single neuron has three inputs, and each of them accept control signal u_1, u_2 and u_3 of the three self-tuning PID controllers. The output u^* of each single neuron is used as control signal, which is compensated , to feed multi variable system. The decoupling of the speed and tension is finally realized by correcting weights of neuron [9].

The algorithm of neuron decoupling compensator in Figure.3 is:

$$\begin{cases} u_j^*(k) = \sum_{j=1}^{3} w_{ij} u_j(k) \\ w_{ij}(k+1) = w_{ij}(k) + \eta(\bar{u}_i^*(k) - u_i^*(k)) u_j(k) \end{cases} \tag{16}$$

The initial value of weight w_{ij} is selected as $\begin{cases} w_{ij} = 1 (i = j) \\ w_{ij} = 0 (i \neq j) \end{cases}$, which equals to without decoupling status. η is learning rate. $u_j^*(k)$ is actual output and $\bar{u}_i^*(k)$ is expected output of neuron.

$J_i = \frac{1}{2}(r_i(k) - y_i(k))^2$ is regarded as the objective function. In order to make J_i minimum, gradient descent method is adopted to search, so the calculation formula of weight coefficient is:

$$\begin{cases} w_{ij}(k+1) = w_{ij}(k) + \eta(r_i(k) - y_i(k)) \operatorname{sgn} \frac{y_i(k+1) - y_i(k)}{u_i^*(k) - u_i^*(k-1)} u_j(k) (i \neq j) \\ w_{ij} = 1 \qquad (i = j) \end{cases} \tag{17}$$

4. Experiment Results of the Multi Induction Motor Synchronous Drive System

4.1. Introduction of the Experimental Hardware System

The experiments are carried out on multi induction motor synchronous control equipment developed by ourselves [5] [10]. The experimental platform are mainly composed of common load, three MMV inverters, three AC motors of 380V/50Hz/2.2kW, upper computer, S7-300 PLC, photoelectric encoder, tension sensor and other equipments. Figure.5 is the structural diagram of multi motor synchronous experimental platform.

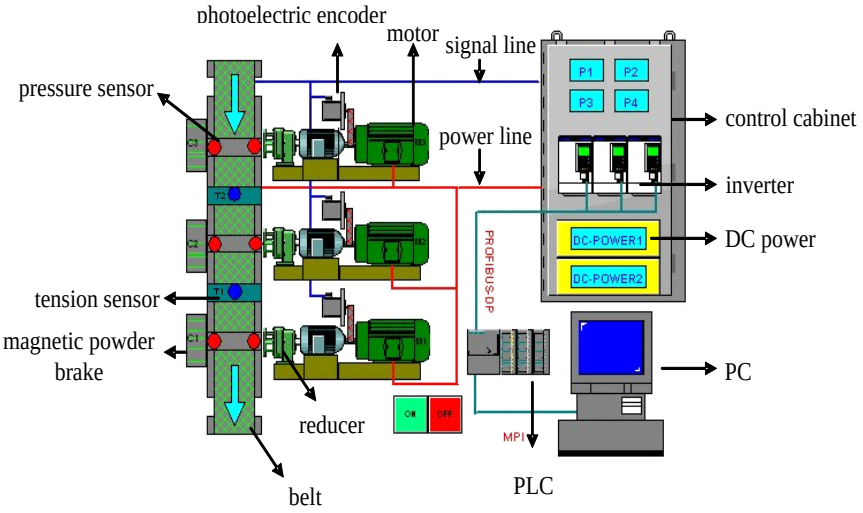

Figure 5. Multi Motor Synchronous Drive System Experimental Platform

4.2. PLC Hardware Configuration

A 315-2DP is selected as the CPU of S7-300PLC. It has MPI and Profibus-DP communication ports. It also has medium and large scale program storage capacity and data structure, and strong treatment ability to floating-point operation. Therefore, it can meet the requirements of neural network control algorithm, which has a lot of floating-point operation. A power module PS307 10A, supplied by ac 220V, provides four-channel 24V dc power supply. A digital input module (DI16×DC24V, Alarm) realizes switch signal start-stop control. A analog input/output module(AI4/AO4×14/12Bit) realizes tension signals collection. A high speed counter module FM350-1 realizes the count of pulses emitted by photoelectric encoder. The main hardware type in the PLC control system are shown in Table 1.

Table 1. Main Hardware Type of PLC Control System

name	type	quantity
CPU	6ES7 307-1KA00-0AA0	1
Power supply	6ES7 315-2AG10-0AB0	1
Memory card	6ES7 953-81M20-0AA0	1
digital input	6ES7 321-7BH01-0AB0	1
analog input/output	6ES7 335-7HG01-0AB0	1
counter	6ES7 350-1AH03-0AE0	1
frame	6ES7 390-1AF30-0AA0	1
inverter	6SE9221-0BC40	3

4.3. Parameters Measurement

4.3.1. Speed Sample

Siemens high speed counter module FM350-1 is adopted to count the pulses emitted by photoelectric encoder. In this experimental system, the type of photoelectric encoder is YGM-615, whose working voltage is 5V±5%. 2048 pulses are emitted by photoelectric encoder during every round. M count method is adopted in the experiment. Then, the calculation formula of speed and electric angular velocity can be obtained as follows:

$$\omega = \frac{2\pi \times \frac{c}{e}}{T} \tag{16}$$

$$n = \frac{60 \times \omega}{2\pi} = \frac{60 \times \frac{c}{e}}{T} \tag{17}$$

Where,

n : the speed of motor($r / \min$),

ω : electric angular velocity(rad / s),

T : count period, T =0.1s ,

c : pulse count value of high speed counter module,

e : pulse number emitted by photoelectric encoder during every round.

Then, the final calculation formula of speed is:

$$n = 0.29296875 \times c \quad (r / \min) \tag{18}$$

4.3.2. The Detection of Tension Displacement

Two sets of SL100 sensor are adopted to detect the belt tension between the two adjacent motors, whose working voltage is 12V, output voltage is 1~5V, and range is 50kg. Concrete calibration data are shown in Table 2, and the mathematical relation can be expressed approximately shown in Figure 6.

Table 2. Tension-Voltage Calibration Data Table

range	0.00	10	20	30	40	50	Kg
progress	1.000	1.803	2.596	3.400	4.201	5.001	V
return	1.000	1.801	2.596	3.400	4.200	5.000	V
standard value	1.000	1.800	2.596	3.400	4.200	5.000	Kg

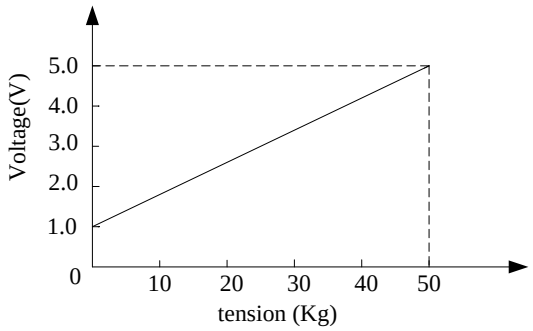

Figure 6. Tension-Voltage Calibration Chart

4.4. The Design of Structured Program

There are three programming methods in STEP7, linear, modularization and structured programming. The third method is adopted in this paper. A complex automation task is usually deposed into small task blocks (FC or FB) which are able to reflect process technology and function, or reusable, then OB1 is used to call these task blocks. This programming idea is in good agreement with design requirement of the subject programming, so structured programming is introduced. The program structure diagram

of the multi motor synchronous drive system is shown in Figure 7. Ladder diagram programming is adopted in industrial software STEP7 V5.4. The software of control system is designed with structural program language, and the program flowcharts are shown in Figure 8 and Figure 9.

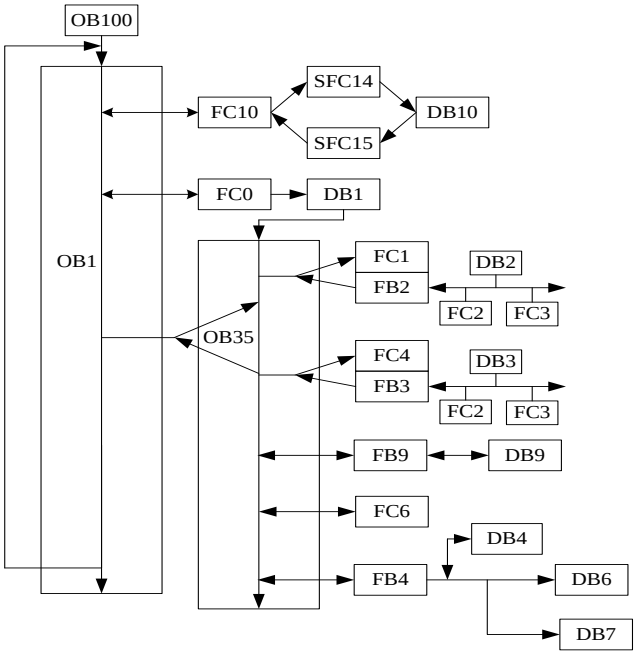

Figure 7. Program Structure Diagram of the Multi Induction Motor System

The main task blocks in Figure 7 are listed in Table.3.

Table 3. Blocks in the Project

Block	Function description
OB1	main program circulation
OB35	circulation interruption, used in process PID
OB100	warm start
FC0	system function of high speed counter
FC1,FC4	set induction motor speed and belt tension
FC6	convert speed into frequency
FC10	inverter communication
FB2, FB3	self-tuning PID based on DRNN algorithm
FB4	file speed and tension sampling data
FB9	neuron decoupling compensation algorithm
DB1	sharing data block of FC0
DB2, DB3, DB4, DB9	instance data block of FB2, FB3, FB4, FB9,
DB6,DB7	sharing data block for saving actual speed and tension
DB10	sharing data block for inverter communication
UDT1	user defined data block of high speed counter
SFC14	read data from Profibus slave station
SFC15	write data to Profibus slave station

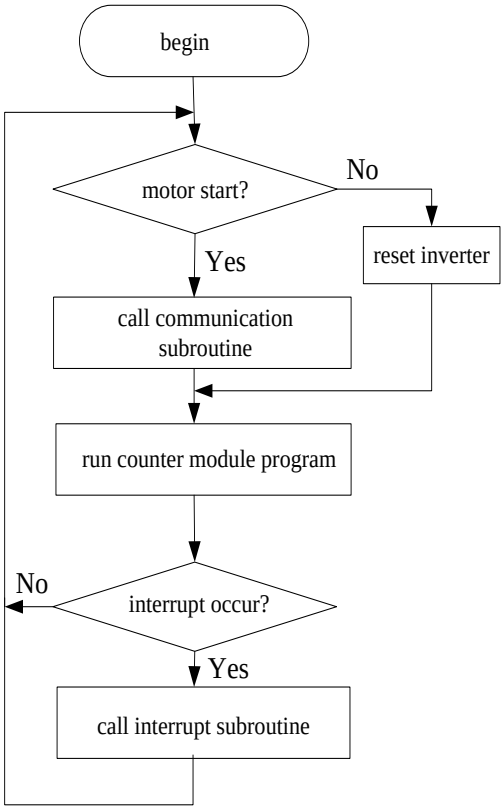

Figure 8. The Flowchart of OB1

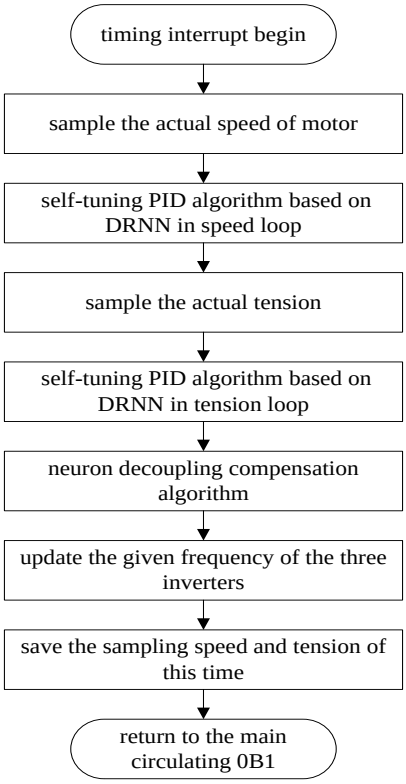

Figure 9. The Flowchart of OB35

5. Experiment Wave and Its Analysis

5.1. Load Experiment

At first, the speed of 1#motor ω_{r1}^{*} is given 150r/min, F_1^{*} is given 10kg and F_2^{*} is given 12kg. After free-load start, load increases at 80 second and decreases at 120 second, speed and tension response curves of multi motor system are shown in Figure.10. As can be seen, neuron network control can make corresponding control adjustment according to load changes, so as to keep speed and tension constant furthest with no influence of load changes.

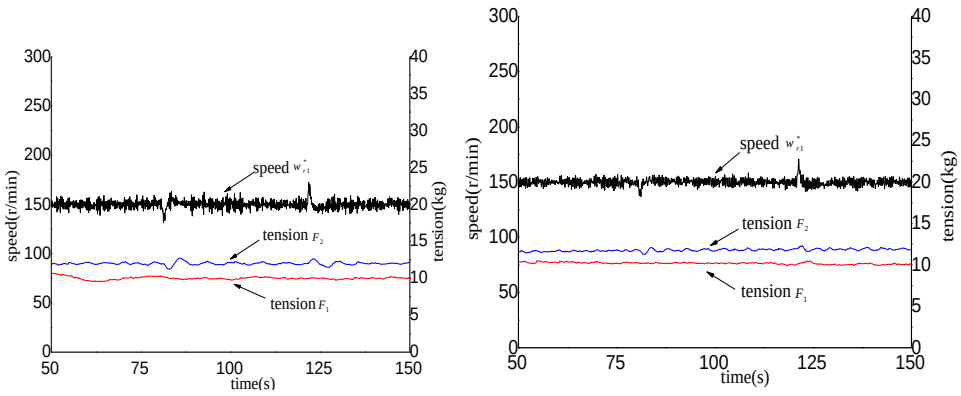

(a) PID control **(b) neuron network control**

Figure 10. The Response of Sudden Load Change

5.2. Decoupling Experiment

Decoupling effect is the main index to measure the control scheme of multi motor synchronous drive system. Taking the system response of sudden speed changes as example, the decoupling effect with PID control and neuron network control are compared. At first, the speed of 1#motor ω_{r1}^{*} is given 300r/min, F_1^{*} is given 10kg and F_2^{*} is given 12kg. After free-load start, the given speed ω_{r1}^{*} increases or decreases at 100 second, experiment results are shown in Figure.11 and Figure.12. As can be seen, the better decoupling control of speed and tension is realized with neural network control method. In contrast to PID control, it can reduce the influence of speed variation on tension.

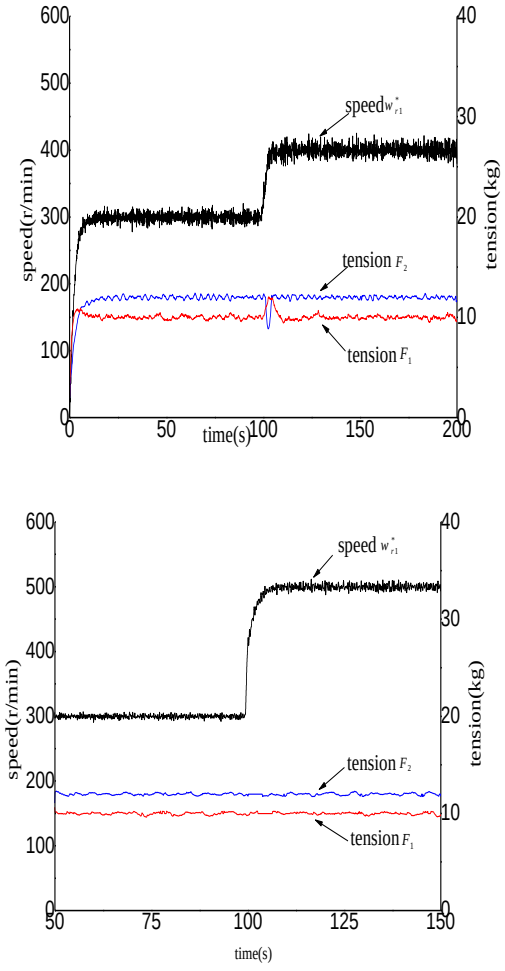

(a) PID control **(b) neuron network control**

Figure 11. The Response of Speed Sudden Increase with Constant Tension

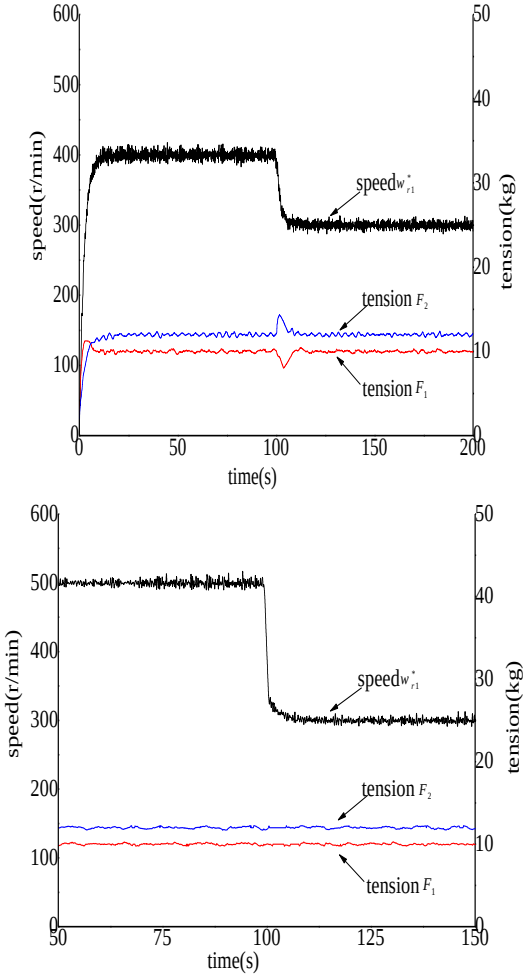

(a) PID control **(b) neuron network control**

Figure 12. The Response of Speed Sudden Decrease with Constant Tension

5.3. Tracking Experiment

At first, the speed of 1#motor ω_{r1}^* is given 300r/min, and it varies from 300r/min to 600r/min in the form of triangular wave after 40 second. The response of speed tracking triangular curves are shown in Figure.13. And the response of speed tracking single period triangular curves are shown in Figure.14. As can be seen from Figure.13(a) and Figure.14(a), the response to the output speed of 1#motor are following triangle waves, appearing a certain error, but in Figure.13(b) and Figure.14(b), the error of both almost is zero.

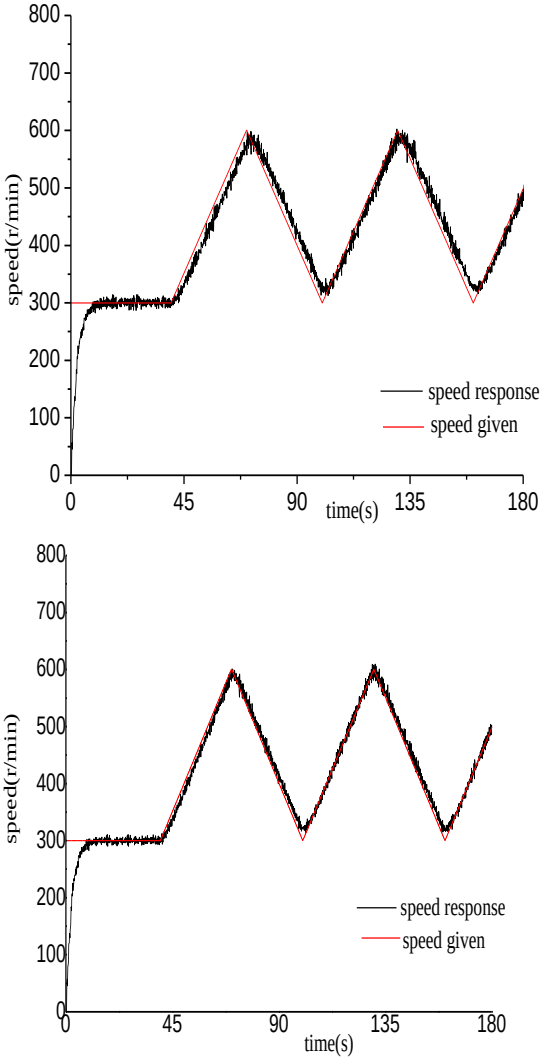

(a) PID control **(b) neuron network control**

Figure 13. The Response of Speed Tracking Triangular Curve

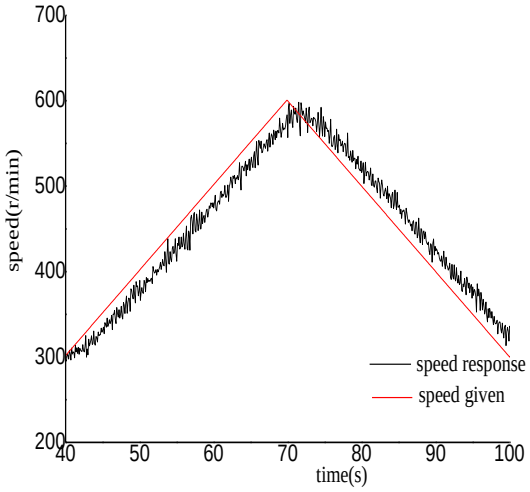

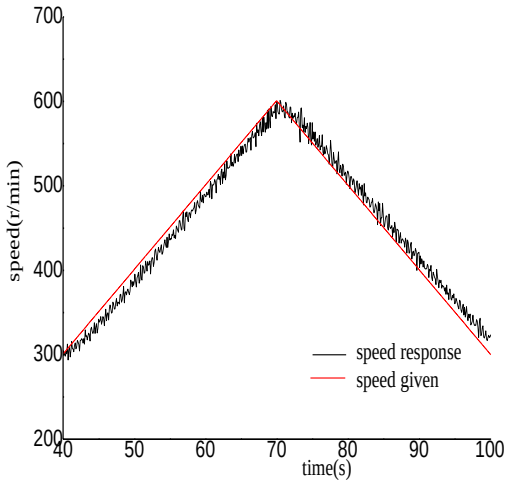

(a) PID control **(b) neuron network control**

Figure 14. The Response of Speed Tracking Single Period Triangular Curve

At first, the speed of 1#motor ω_{r1}^{*} is given 600r/min, and it varies from 600r/min to 800r/min in the form of square wave after 40 second. The response of speed tracking square curves and the local amplification curves are shown in Figure.15 and Figure.16. As can be seen from the curves, neural network control has faster response and higher steady precision.

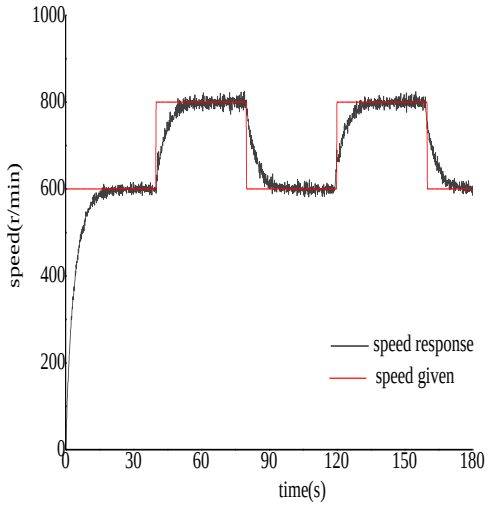

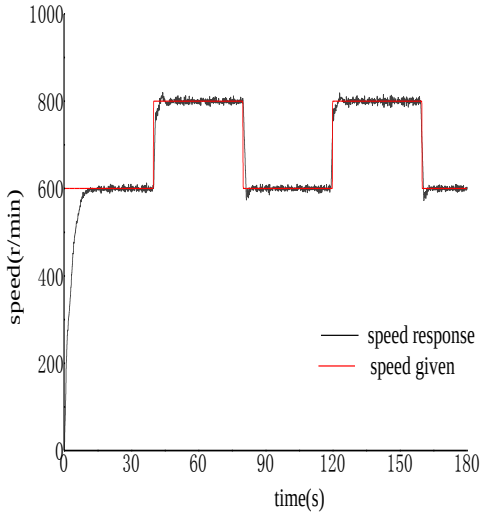

(a) PID control **(b) neuron network control**

Figure 15. The Response of Speed Tracking Square Curve

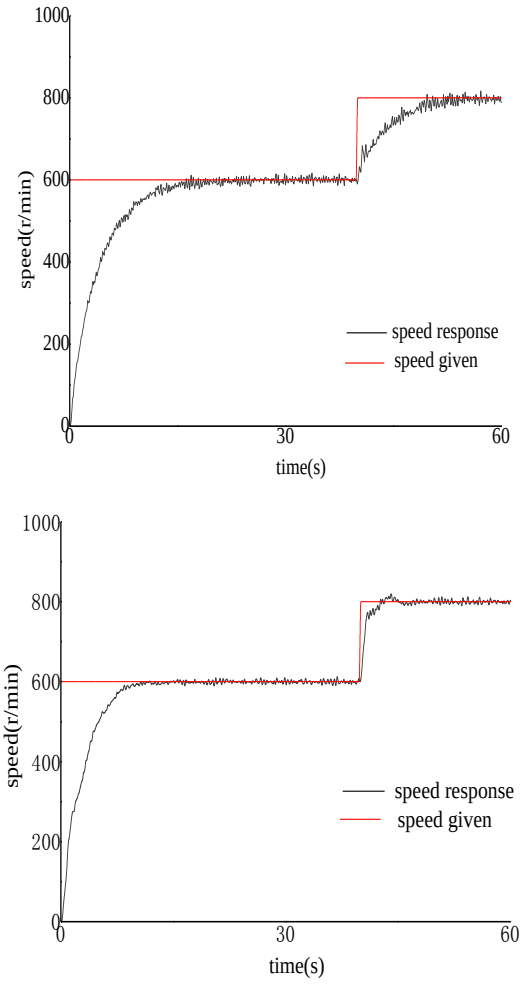

(a) PID control **(b) neuron network control**

Figure 16. The Response of Speed Tracking Square Local Amplification Curve

6. Conclusion

This paper aiming at multi motor synchronous drive system which is multi variable, nonlinear, and coupling, presents a neural network compound controller composed of neuron decoupling compensator and self-tuning PID control method based on multi-variable decoupling and intelligent control theory. It finally realizes the synchronous control of the system based on S7-300 PLC experiment platform. This method is proved to be applied into the synchronous control of three motor drive system, so a new control way of three motor system is presented. The project is further studied by increasing tension self-tuning PID controllers and the dimensions of neuron decoupling compensator, and the authors find that the method can be extended to the usual multi motor synchronous drive system($n \geq 3$), which can satisfy the requests of the actual production.

Acknowledgements

This work was supported in part by the National Natural Science Foundation of China under Grant 51507150 and 51407153.

References

[1] S. H. Song and S. K. Sul, "A new tension controller for continuous strip processing Line", IEEE Transactions on Industry Applications, vol.36, no.2, **(2000)**, pp.633–639.
[2] H. Zhang and G. H. Liu, „Decoupling control of artificial neural network inverse system in AC variable frequenly induction motor system", Journal of Jiangsu University Natural Science Edition, vol.23, **(2002)**, pp. 88-91.
[3] C. Chen, "Neural network control of induction motor speed control system", International Journal of Control and Automation, **(2014)**, vol.7, no.10, pp.243-254.
[4] X. Z. Dai and G. H. Liu, "The neural network inverse control of the constant ratio of voltage and frequency adjusting speed system", Chinese Electrical Engineering College Journal,vol.25, no.7, **(2005)**, pp.109–114.
[5] X.Q. Liu and L. Tang, "Three-motor synchronous control system based on fuzzy active disturbances rejection system", Electric machines and control, vol.17, **(2013)**, pp.104-109.
[6] J. Z. Zhang and G. H. Liu, "Multi-model identification to multi-motor synchronous system", Machines and Control, vol. 13, no. 1, **(2009)**, pp.138-142.
[7] P. Jiang, Z. J. Li and W. P. Liang, "A decoupling algorithm based on neuron", Journal of North China Electric Power University, vol.27, no.2, **(2004)**, pp.47-51.
[8] Z. H. Cui, X. J Cai and J. C. Zeng, "PID-controlled particle swarm optimization", Journal of Multiple-Valued Logic and Soft Computing, vol.16, no.6, **(2010)**, pp.585-610.
[9] L. Dong and Y. Bai, "Neural decoupling control for multi variable system", Modern Electric Power, vol.16, no.1, **(1999)**, pp.11–15.
[10] C. Chen and G. W. Hu, "Fuzzy PID control of induction motor speed regulating system", International Journal of Wireless and Mobile Computing, vol. 6, no. 4, **(2013)**, pp.321-330.

Authors

Chong Chen, he was born in Jiangsu Province, China, in 1982. He received his master degree in Electrical Engineering from Jiangsu University in 2008. He is currently working at School of Electrical Engineering, YanCheng Institute of Technology, China. His current research interest include motion control and power electron application.

Simin Peng, he was born in Hunan province, China, in 1980. He received the B.S degree in automation from Xiangtan University, Xiangtan, China, in 2003, and M.S. degree in 2008, and Ph.D degree in electrical engineering from Shanghai Jiao Tong University in 2013. He is currently working at Yancheng Institute of Technology. His research interests include wind power, microgrid, battery energy storage system and battery manage system.

Zhilei Yao, he was born in Jiangsu Province, China, in 1981. He received the B.S., M.S., and Ph.D. degrees in electrical engineering from Nanjing University of Aeronautics and Astronautics, Nanjing, China, in 2003, 2006, and 2012, respectively.He is with the School of Electrical Engineering, Yancheng Institute of Technology, Yancheng, China, where he is currently an Associate Professor. He holds fourteen patents, and is the author or coauthor of more than 60 technical papers. His current research interests include dc–dc converters, inverters, and distributed power generation